Observations of Planetary Mixed Rossby–Gravity Waves in the Upper Stratosphere

WILLIAM J. RANDEL, BYRON A. BOVILLE AND JOHN C. GILLE

National Center for Atmospheric Research, Boulder, Colorado*

(Manuscript received 10 February 1990, in final form 1 August 1990)

ABSTRACT

Observational evidence is presented for planetary scale (zonal wave number 1–2) mixed Rossby-gravity (MRG) waves in the equatorial upper stratosphere (35–50 km). These waves are detected in Limb Infrared Monitor of the Stratosphere (LIMS) measurements as coherently propagating temperature maxima of amplitude 0.1–0.3 K, which are antisymmetric (out of phase) about the equator, centered near 10°–15° north and south latitude. These features have vertical wavelengths of order 10–15 km, periods near 2–3 days, and zonal phase velocities close to 200 m s^{-1}. Both eastward and westward propagating waves are found, and the observed vertical wavelengths and meridional structures are in good agreement with the MRG dispersion relation. Theoretical estimates of the zonal accelerations attributable to these waves suggest they do not contribute substantially to the zonal momentum balance in the middle atmosphere.

1. Introduction

Mixed Rossby–gravity (MRG) waves were first documented in meridional wind measurements in the tropical upper troposphere/lower stratosphere by Yanai and Maruyama (1966). This and subsequent work by these authors showed that westward propagating disturbances of period ~ 5 days with zonal scales of order 10 000 km (zonal wave 4) and vertical wavelengths of 4–8 km are regularly observed in the tropical Pacific. They are frequently referred to as Yanai waves. Wallace (1973) provides a review and reference index for these observations. The vertical propagation of these waves is believed to provide an important westward momentum source for the quasi-biennial oscillation of the zonal wind in the lower stratosphere (Holton and Lindzen 1972).

Boville and Randel (1991) have recently analyzed the properties of equatorial waves in several high-resolution troposphere–stratosphere general circulation model simulations. The focus of that work was to study the effects of model resolution on equatorial wave structure. An interesting sidelight to that study was the observation that modeled MRG wave spectra in the middle and upper stratosphere were dominated by planetary waves (zonal waves 1–2). This apparently occurs in the model because of the selective absorption of shorter horizontal (and vertical) scale MRG waves in the lower stratosphere.

The purpose of this paper is to document the existence of planetary-scale MRG waves in the upper stratosphere, using temperature observations from the Limb Infrared Monitor of the Stratosphere (LIMS). Because of the high frequency of these waves (2–3 days), a new mapping of the LIMS data is used in which the zonal Fourier coefficients are output twice daily. LIMS temperature power spectra show planetary wave features similar to those observed in the model previously mentioned. In particular, the LIMS spectra exhibit power maxima near 15° north and south latitude with an out of phase horizontal structure characteristic of MRG waves. The observed vertical wavelengths and meridional structures are in good agreement with the MRG dispersion relation. Theoretical estimates of the forcing of the zonal-mean flow due to these MRG waves are made, and the results suggest they do not contribute appreciably to the zonal momentum balance.

2. Data and results

a. Background

MRG waves are most clearly identified as equatorially-centered, latitudinally evanescent amplitude maxima in the meridional wind field. Figure 1a shows a latitude–frequency section of wave 1 spectral power density for the meridional wind at 3 mb from the model results of Boville and Randel (1991); zonal wave 1 dominates the variance at this level in the model. The model is sampled twice daily during 120 days covering December–March, identical to the sampling for the

* The National Center for Atmospheric Research is sponsored by the National Science Foundation.

Corresponding author address: Dr. William J. Randel, National Center for Atmospheric Research, P.O. Box 3000, Boulder, CO 80307-3000.

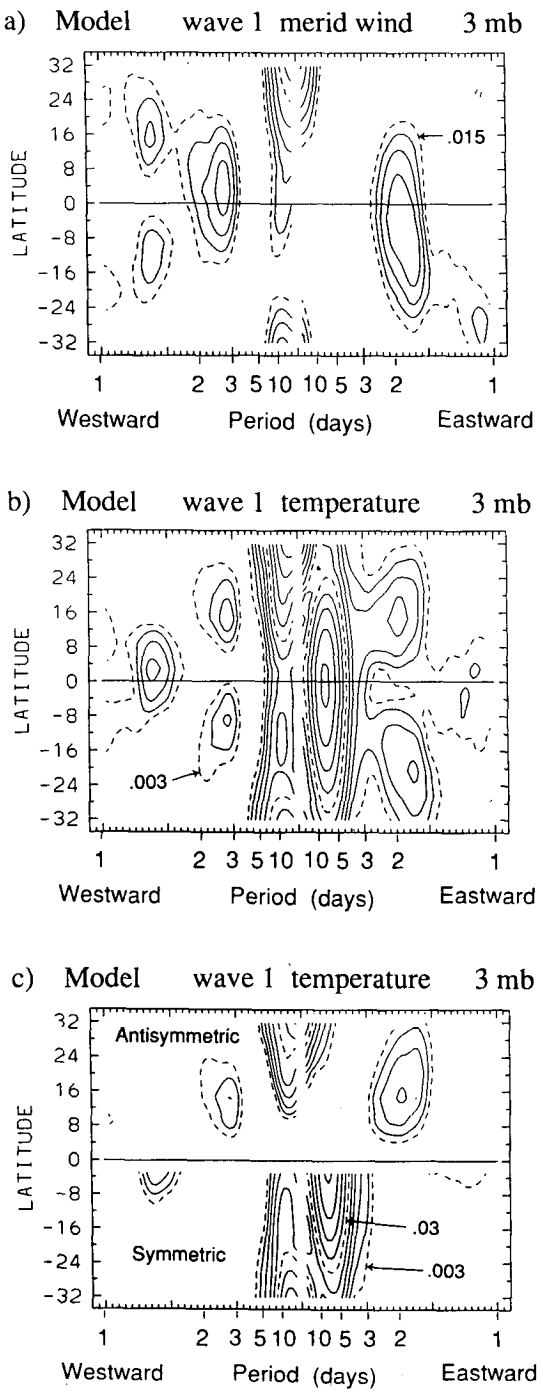

FIG. 1. (a) Latitude–frequency power spectral density at 3 mb for zonal wave 1 meridional wind from the model results of Boville and Randel (1991). Units are $m^2\ s^{-2}\Delta\omega^{-1}$, with $\Delta\omega$ the unit frequency interval of $(2\pi/120$ days). Equatorially centered maxima for eastward and westward periods near 2–3 days are signatures of zonal wave 1 MRG waves. (b) 3-mb zonal wave 1 temperature power spectral density from the model data. Units are $°K^2\Delta\omega^{-1}$. (c) Power spectral density for antisymmetric (top half of panel) and symmetric (bottom half of panel) components of temperature in (b). In these and the following power spectra, contours are equally spaced logarithmically with contour intervals in ratios of 1.0:1.6:2.5:4.0:6.3:10.0, etc. The first contour of each decade is noted as a dashed line and labeled.

LIMS data. Spectral calculations are identical to the analyses applied to LIMS data later discussed.

Figure 1a shows both eastward and westward propagating power maxima centered on the equator, near periods of 1.8 and 2.7 days, respectively, and these are signatures of MRG waves (i.e., meridional winds maximizing at the equator with a latitudinally evanescent amplitude structure; see Andrews et al. 1987, section 4.7). The eastward propagating modes are shifted somewhat southward and the westward modes somewhat northward in Fig. 1a, probably because of the substantial northward shear of the zonal-mean zonal wind. Also seen are 1.3-day westward (and weak 1.1-day eastward) maxima centered near 15° (and 25°) north and south latitude, which are associated with equatorially trapped inertio–gravity waves with meridional quantum index $n = 1$ (meridional winds out of phase across the equator); see Boville and Randel (1991) for further details of these modes in the model.

Figure 1b shows 3-mb wave 1 temperature power from the model, i.e., at the same level as the meridional wind spectra in Fig. 1a. There is a strong equatorially centered eastward power maximum near a period of 7.5 days, this being evidence of Kelvin waves in the model (see Boville and Cheng 1988; Boville and Randel 1991). Of more importance here are the temperature maxima centered near 10°–20° north and south, near periods of 2–3 days, for both eastward and westward propagating components; these are the temperature perturbations associated with the equatorially centered meridional wind maxima in Fig. 1a. Note the order of magnitude difference between the power maximum in the Kelvin mode and those associated with the MRG waves. Because of this order of magnitude difference, temperature power spectra are plotted using contour intervals which increase logarithmically (as noted in Fig. 1b). Temperature fluctuations associated with the $n = 1$ inertio–gravity waves are predominantly centered near the equator in Fig. 1b.

Temperature fluctuations associated with MRG waves are out of phase (antisymmetric) about the equator, while Kelvin wave and $n = 1$ inertio–gravity wave signatures are in phase (symmetric). The antisymmetric and symmetric components at latitude ϕ are written as:

$$T_A(\phi) = [T(\phi) - T(-\phi)]/2 \qquad (1a)$$

$$T_S(\phi) = [T(\phi) + T(-\phi)]/2. \qquad (1b)$$

Figure 1c shows model spectral power for temperatures decomposed into antisymmetric and symmetric components. This separation clearly distinguishes the MRG modes (antisymmetric) from the Kelvin wave (symmetric). It is this signature of antisymmetric temperature power at high frequencies that is shown here in LIMS data as evidence of planetary MRG waves in the atmosphere.

b. *High-resolution mapped LIMS data*

The LIMS experiment operated aboard the Nimbus-7 satellite from 25 October 1978 to 28 May 1979. A comprehensive description of the experiment can be found in Gille and Russell (1984). One hundred twenty days of LIMS data are used here, covering 1 December 1978–30 March 1979. The archival set of LIMS temperature retrievals, so-called V5 data, are analyzed here. Salby et al. (1984) and Hitchman and Leovy (1988) studied a preliminary version of LIMS retrievals, labeled V4, to document Kelvin waves in LIMS temperatures. Qualitatively, V4 and V5 LIMS temperature data are similar in the tropics, with V4 retrievals accentuating features with strong vertical variations. The V4 data reveal MRG signatures similar to those shown in V5 data here, with amplitudes approximately 1–2 times as large. However, signal-to-noise ratio (as measured by the coherence squared statistic) is significantly stronger for MRG waves in the V5 data, and hence those data are presented here.

The archival set of LIMS V5 temperatures consists of daily zonal Fourier coefficients every 4° latitude on the following standard pressure levels: 100, 70, 50, 30, 16, 10, 7, 5, 3, 2, 1.5, 1.0, 0.7, 0.5, 0.4, 0.2, and 0.1 mb. Horizontal mapping is performed based on the Kalman filter sequential estimation technique (Rodgers 1976). Space–time spectral analyses performed on these daily data revealed MRG signatures very similar to those shown here. However, because the period of the waves in question (2–3 days) was very close to the Nyquist period for daily data (2 days), there was a possibility that significant aliasing of the spectral estimates could occur. It was therefore decided to remap the profiles and output the fields every 12 hours, and hence push the Nyquist period to one day. Furthermore, because of the short vertical scales found here, the vertical resolution of the mapped data has been doubled over that used in the original archive, resulting in data at levels spaced about 1.5 km apart.

c. *Spectral analyses*

Eastward–westward power spectral density estimates are calculated following the method described in Hayashi (1982). Time spectra are calculated by direct Fourier transform, and the spectral estimates at frequency ω_0 are smoothed in frequency using a normalized Gaussian spectral window of the form $W(\omega - \omega_0) = e^{-[(\omega-\omega_0)/\Delta\omega]^2}$, with $\Delta\omega = 5$. This spectral bandwidth was chosen to give good balance between spectral resolution and stability, and is shown in Fig. 2a. Also calculated were the band-averaged statistics representing individual wave modes identified in the power spectra; these band averages are calculated by integrating the Gaussian-weighted cross-spectral estimates centered on the chosen frequency interval. Wave amplitude is calculated as the square root of twice the spectral power. Spectral coherence squared and phase are calculated as in Hayashi (1982).

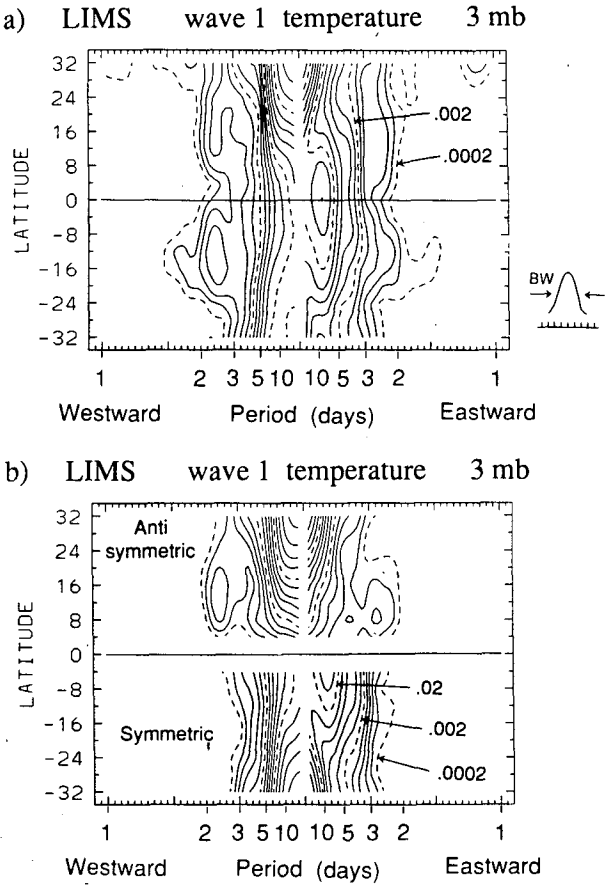

FIG. 2. (a) Latitude–frequency power spectral density for LIMS temperature data for zonal wave 1 at 3 mb. (b) Shows spectra for temperature separated into components antisymmetric and symmetric about the equator. Units are $°K^2\Delta\omega^{-1}$. The spectral bandwidth (BW) is indicated in (a).

d. *MRG waves in LIMS data*

Figure 2a shows a latitude–frequency section of LIMS temperature spectral power density for zonal wave 1 at 3 mb. Figure 2b shows the decomposition of these data into components symmetric and antisymmetric about the equator (Eqs. 1a,b). There is a strong equatorially centered, latitudinally evanescent power maximum for eastward moving waves centered near a period of 10 days. This feature is primarily symmetric in character, and is evidence of Kelvin modes in the LIMS data as first documented by Salby et al. (1984). Careful inspection of Fig. 2a shows that additionally there are temperature variance maxima centered at approximately 15° north and south latitude at both eastward and westward periods near 2–3 days. The westward moving feature is particularly clear in the total temperature spectra (Fig. 2a); the fact that it

is primarily antisymmetric is highlighted in Fig. 2b. The antisymmetric spectra (Fig. 2b) also show an eastward maximum centered near 8°–12° latitude, but in contrast to the westward moving waves there is as much or more symmetric than antisymmetric power (because of their proximity to the eastward moving Kelvin waves). The spectra in Fig. 2 are qualitatively similar to the model temperature power spectra (Figs. 1b,c). LIMS temperature power spectra such as Fig. 2 suggest evidence of wave 1 MRG modes with period near 3 days near 30 km; however, the signal is tenuous and not coherent over many adjacent pressure levels, and we focus mainly on the stronger features observed in the upper stratosphere.

Figure 3 shows vertical sections of antisymmetric temperature power at 12° latitude for zonal waves 1 and 2. Wave 1 antisymmetric power (Fig. 3a) exhibits spectral maxima for westward moving waves centered near periods of 2.4 days with separated peaks near 40 and 50 km. Wave 1 also shows an eastward maximum near 2.4 day period with a more continuous vertical amplitude structure over 40–50 km. Wave 2 (Fig. 3b) shows a westward maximum positioned similarly in frequency to that found for wave 1, near 45 km. This wave 2 feature has a vertical wavelength near 15 km, nearly identical to that for wave 1 (whose vertical structure is discussed later). Because wave 2 antisymmetric power peaks at an altitude where there is a minimum in that for wave 1, and has a vertical wavelength identical to that of wave 1, it is concluded that the spectral peak in wave 2 does not identify a distinct mode but represents the same physical feature as wave 1. The physical feature being represented by the spectra is probably somewhat localized in longitude. The degree of localization may change in the vertical in response to changes in the background shears, among other things. As a result, the feature may project more strongly onto wave 2 than wave 1 at different altitudes. Wave 2 is not discussed further here.

Figure 4 shows meridional cross sections of temperature amplitude for the westward and eastward propagating wave 1 modes identified in Figs. 2–3 (the spectral bands are indicated in Fig. 3a). Temperature maxima are of the order 0.1–0.3°K. The westward mode shows several maxima and minima in height, and a suggestion of some northward shifting of the patterns near 45–50 km. Amplitude variations in the vertical may be partly due to a stronger projection of the physical feature onto zonal wave 2 in this frequency band at certain heights (i.e., Figs. 3a,b and discussion above). Such structure could also result from sampling considerations or represent true atmospheric structure (related to shears in the background winds, for instance); Salby et al. (1984) found similar strong vertical amplitude variations for Kelvin wave signatures in LIMS data. The northward shift seen in Fig. 4a is also seen in the westward MRG mode in the model results (Figs. 1a,b), and may be due to the strong northward shears of the zonal-mean wind observed in the tropical upper stratosphere (Boyd 1978); note the zonal wind profile for this time period shown in Fig. 18 of Salby et al. (1984). The eastward mode in Fig. 4b does not show the vertical amplitude variations or meridional shifting seen in the westward mode.

The vertical phase structures of the westward and eastward antisymmetric modes are shown in Fig. 5. These phases were calculated by considering only the antisymmetric temperatures at 12° latitude, integrated over the appropriate spectral bands. Quasi-regular phase progression with height is found over much of the middle stratosphere in Fig. 5; the westward propagating mode tilts westward with height with a vertical

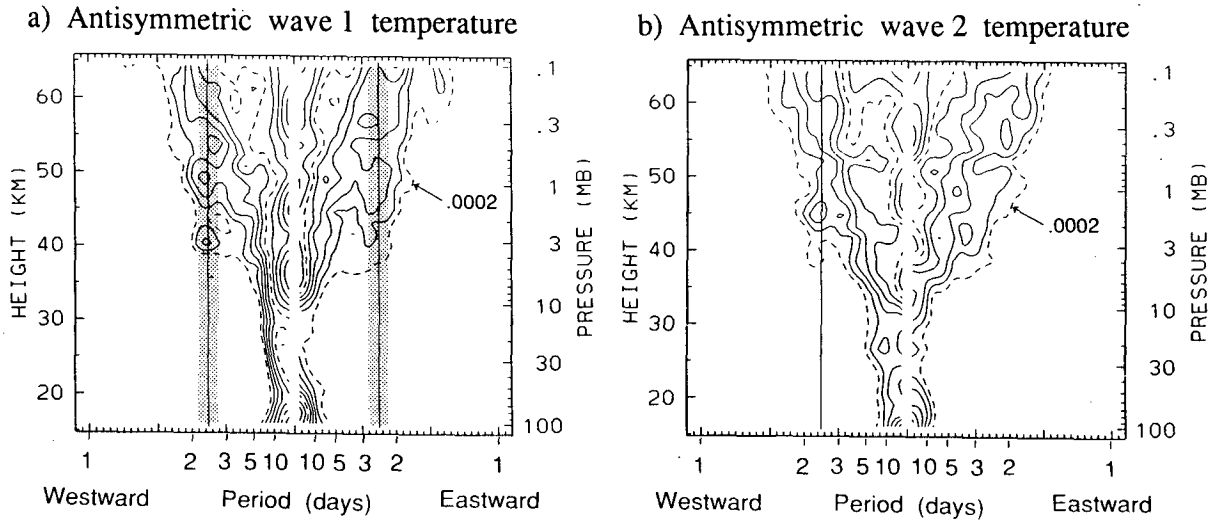

FIG. 3. Height–frequency power spectral density of asymmetric temperature at 12° latitude for zonal waves 1 (left) and 2 (right). Vertical lines with shading denote the spectral features and associated bandwidths analyzed in Figs. 4–5.

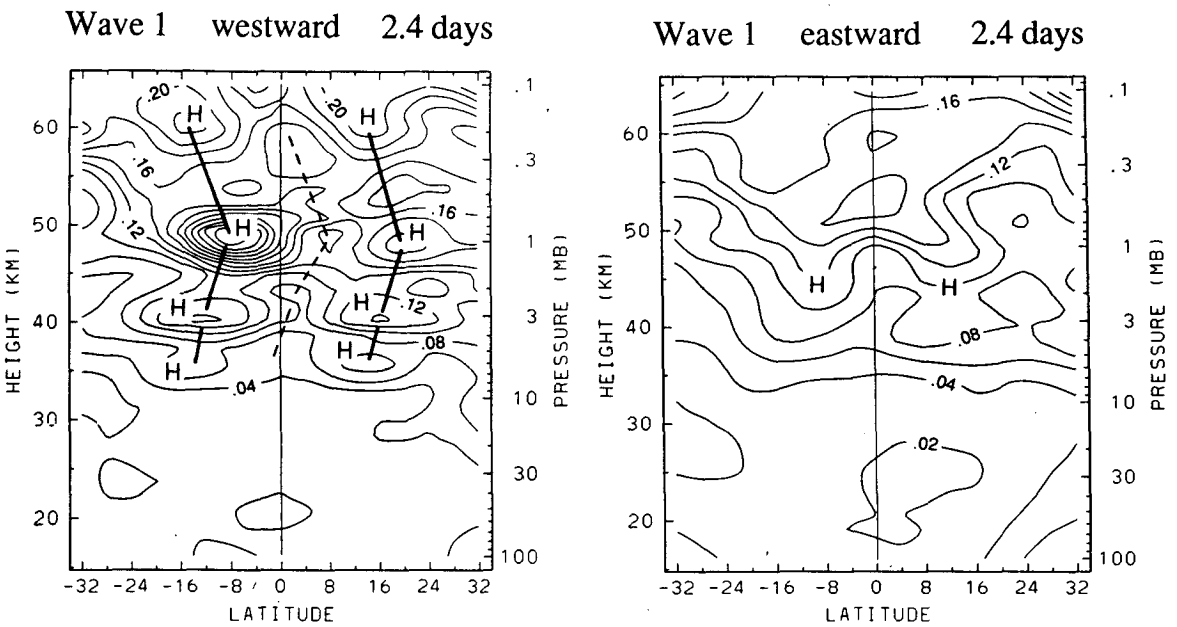

FIG. 4. Meridional cross sections of temperature amplitude for the westward and eastward propagating zonal wave 1 spectral features identified in Fig. 3a. No separation between symmetric and antisymmetric components has been made here. Contour interval is 0.02°K. Amplitude maxima associated with MRG waves are noted by 'H's.

wavelength near 15 km, while the eastward propagating mode tilts eastward with height with a wavelength near 9 km. Irregular phase variations are found in Fig. 5 in the upper and lower regions of analysis; here, the modes are not statistically coherent and calculated phase values have large uncertainties.

The observed vertical wavelengths derived from Fig. 5 are tabulated in Table 1. Also included in Table 1

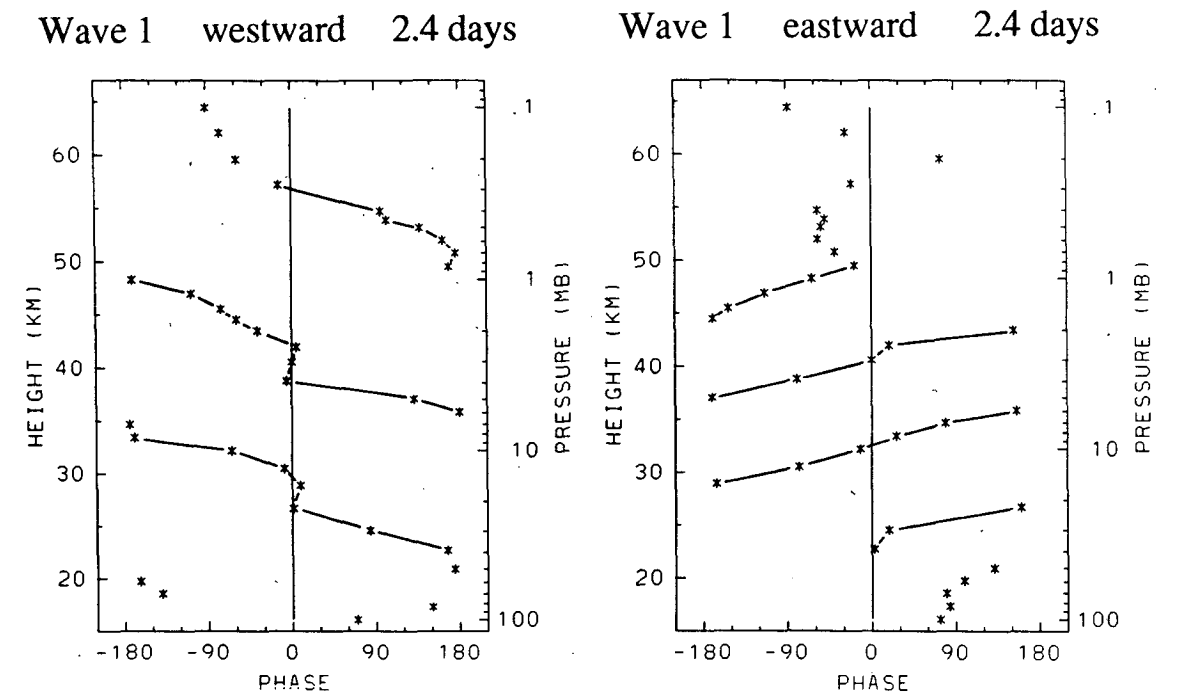

FIG. 5. Vertical phase structure for the westward and eastward propagating zonal wave 1 spectral features identified in Fig. 3a, calculated using only the antisymmetric temperatures at 12° latitude. Phase estimates at each analysis pressure level are indicated by '*'s; reference pressure level is 3 mb. Straight lines connect phases over regions where the respective waves are statistically coherent.

TABLE 1. Characteristics of the band-averaged MRG modes shown in Figs. 4–5.

Zonal wave number	Period (days) E = eastward W = westward	Zonal trace speed (m s^{-1})	Observed λ_z (km) (Fig. 5)	Calculated λ_z (km) (Eq. 4)	Calculated vertical group velocity (km day^{-1}) (Eq. 5)
1	2.4 W	−190	13–16	14.4	2.6
1	2.4 E	+190	8–9	9.4	2.2

are vertical wavelengths (λ_z) calculated from the MRG dispersion relation (from Andrews et al. 1987, Eq. 4.7.16):

$$m = -\mathrm{sgn}(\omega) \times N(\beta + \omega k_*)/\omega^2. \quad (4)$$

Here, $m = 2\pi/\lambda_z$ is the vertical wave number, N is the Brunt–Vaisäla frequency (2.2×10^{-2} s^{-1}), β is the planetary vorticity gradient (2.3×10^{-11} m^{-1} s^{-1}), and k_* is the dimensional zonal wave number. This dispersion relation is shown graphically for zonal waves 1 and 2 in Fig. 6. There is overall excellent agreement between the observed and calculated vertical wavelengths for both zonal wave 1 modes in Table 1 (Fig. 6), supporting their identification as MRG modes. Also included in Table 1 are vertical group velocities calculated from

$$Cg_z = \pm\omega^3/N(2\beta + \omega k), \quad (5)$$

(Andrews et al. 1987, Eq. 4.7.18). Values for the planetary MRG waves are of the order of a few kilometers per day.

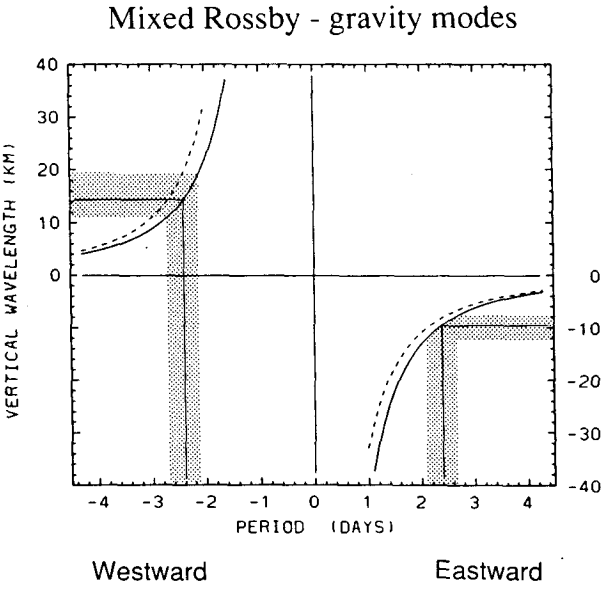

FIG. 6. Dispersion diagram for zonal wave 1 (solid) and 2 (dashed lines) mixed Rossby-gravity waves, from Eq. 3. Negative vertical wavelengths denote eastward phase tilt with height. The straight lines correspond to spectral features identified in LIMS data in Figs. 3–5, and shading denotes the spectral bandwidths used in the calculations here.

The meridional structure of MRG temperature perturbations has a latitudinal dependence of the form

$$T(\eta) = (\text{constant})\eta e^{-1/2\eta^2}, \quad (6)$$

with

$$\eta = (\beta m/N)^{1/2} a\phi$$

a modified latitude coordinate (Andrews et al. 1987, Eq. 4.7.14c). Here, ϕ is latitude and a is the earth radius (6.37×10^6 m). Note that the latitudinal structure in (6) depends on vertical wavelength. Figures 7a,b show plots of (6) using vertical wavelengths of 15 and 9 km, along with antisymmetric temperature amplitudes for the westward ($\lambda_z \sim 15$ km) and eastward ($\lambda_z \sim 9$ km) modes from Fig. 4. The theoretical and observed structures are in reasonable agreement; in particular the eastward ($\lambda_z \sim 9$ km) mode has maxima somewhat nearer the equator and narrower meridional structure than the westward mode. This behavior is also clearly seen in the power spectra in Fig. 2b, and strengthens identification of these features as planetary MRG waves.

3. Influence of planetary MRG waves in the middle atmosphere

Wave-induced zonal accelerations resulting from vertically propagating MRG waves are thought to be important for the easterly acceleration of the QBO in the lower stratosphere (Holton and Lindzen 1972). The most important motions which contribute to that forcing are likely the zonal wave 4, 5-day period features (Yanai waves). The model results of Boville and Randel (1991) suggest that planetary MRG waves are damped by a comparatively small amount in the lower stratosphere, likely due to their much faster vertical group velocities (Cg_z for Yanai waves are near 0.3 km day^{-1}, about one-tenth of the planetary wave values in Table 1). The planetary MRG waves are thus probably not important for the QBO.

A further possibility is that planetary MRG waves contribute to the stratopause or mesopause semiannual oscillations (SAOs). The wave-induced zonal accelerations (wave driving) may be estimated from the Eliassen–Palm (EP) flux divergence $\partial F_z/\partial z$ (Andrews et al. 1987; F_y is negligible here). The quantity F_z is the vertical component of the EP flux:

$$F_z = \rho_0 a \cos\phi[(\hat{f}R\overline{v'T'}/HN^2) - \overline{u'w'}], \quad (7)$$

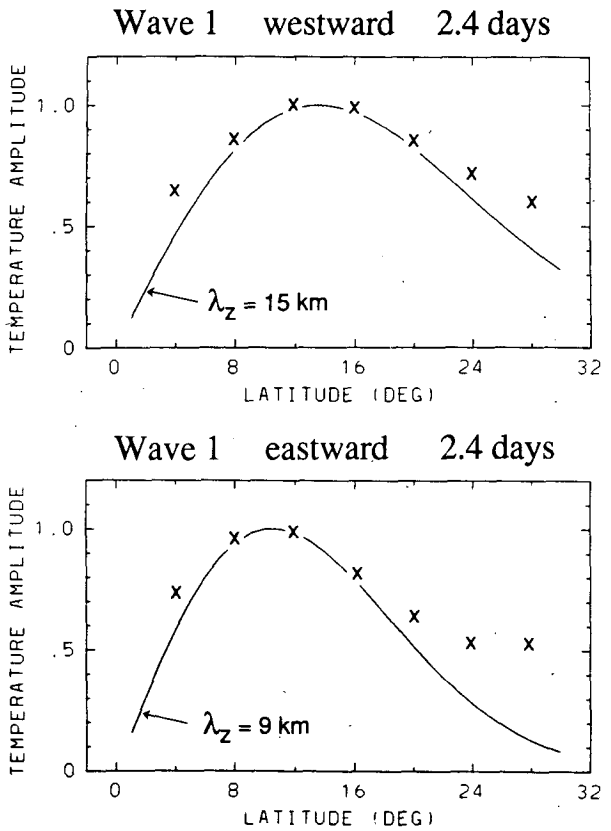

FIG. 7. Meridional structure of temperature amplitudes for MRG waves. 'X's denote antisymmetric temperature amplitudes for the westward and eastward propagating zonal wave 1 features shown in Fig. 4; values are normalized to a maximum value of 1.0. Amplitudes are taken from the 3- and 1-mb levels, respectively, for the westward and eastward modes shown in Fig. 4. Continuous lines denote the functional behavior of Eq. 6 for vertical wavelengths of 15 and 9 km, also normalized to maximum values of 1.0.

where $\hat{f} = 2\Omega \sin\phi - (a\cos\phi)^{-1}\partial(\bar{u}\cos\phi)/\partial\phi$, and other notation standard. For the qualitative discussion here it is assumed the sign of $\partial F_z/\partial z$ is opposite that of F_z, such as would occur for a monotonic decrease in the magnitude of F_z with height above the tropopause; this assumption is verified for Kelvin waves ($\overline{v'T'} = 0$, $\overline{u'w'} > 0$, $\partial F_z/\partial z > 0$) from the calculations of Hitchman and Leovy (1988).

For MRG waves, both terms in (7) are of comparable magnitude, but their effects generally cancel since $\overline{v'T'} > 0$ and $\overline{u'w'} > 0$ (e.g., Holton 1975, p. 136). Neglecting mean wind shear effects, an expression for the latitudinally averaged F_z may be derived which depends only on frequency (ω):

$$\langle F_z\rangle = (\text{constant})(-|\omega|)\left(\frac{\omega k_*}{\beta + \omega k_*}\right). \quad (8)$$

Note that for MRG waves $(\beta + \omega k_*) > 0$; hence from (8), eastward propagating waves ($\omega > 0$) induce $\partial\bar{u}/\partial t > 0$, and westward propagating waves ($\omega < 0$) induce $\partial\bar{u}/\partial t < 0$ in accordance with the general result for internal gravity waves. Thus, planetary MRG waves could conceivably contribute to both easterly and westerly acceleration phases of the SAO.

A relative measure of wave driving for the planetary MRG waves observed here is estimated as follows. An approximate expression may be derived relating the ratio of latitudinally averaged F_z attributable to MRG waves, $\langle F_z\rangle_M$, to that from Kelvin waves, $\langle F_z\rangle_K$:

$$\frac{\langle F_z\rangle_M}{\langle F_z\rangle_K} \approx \left[|\omega_M|\left(\frac{\omega_M k_{*M}}{\beta + \omega_M k_{*M}}\right)\Big/\omega_K\right]\overline{T'^2_M}/\overline{T'^2_K}. \quad (9)$$

Here, the M and K subscripts refer to MRG and Kelvin wave quantities, respectively, and the T'^2 values refer to relative maxima for the respective waves (near 15° and the equator, respectively). The ratio of the temperature variances can be obtained from spectra such as those in Fig. 2, and is of order 0.02 at the 3-mb level. The quantity in brackets in (9) is of order unity for the MRG and Kelvin features in the LIMS data. Hence, the ratio $\langle F_z\rangle_M/\langle F_z\rangle_K \approx 0.02$, and *planetary MRG waves contribute less than one-tenth the body forces attributable to Kelvin waves.* This relatively small MRG wave driving is *not* due to the small temperature amplitudes associated with MRG waves; these small temperatures are simply a result of the mass–wind balance for these tropical motions (if one considered only the meridional wind field, Kelvin waves would appear to have little influence relative to MRG waves). Rather, the relatively small wave driving for MRG waves is ultimately due to the cancellation of the two terms in (7). Hitchman and Leovy (1988) and Hamilton and Mahlman (1988) have suggested that Kelvin waves play a relatively minor role in the stratopause SAO; planetary MRG waves are likely less important yet.

4. Summary and Discussion

Prompted by the model results of Boville and Randel (1991), this study has identified the temperature signal of planetary MRG waves in the tropical upper stratosphere. Space–time spectral analysis of LIMS data shows fast (2–3-day period) temperature variance maxima for zonal waves 1–2 which are antisymmetric about the equator, maximizing near 10°–20° north and south latitude. Band-integrated spectra show that these temperature maxima are statistically coherent and out of phase across the equator. Both eastward and westward propagating modes are identified in LIMS data (Table 1 and Fig. 5), and the observed vertical wavelengths and meridional structures are in good agreement with the MRG dispersion relation. The MRG wave temperature amplitudes observed here are very small (of order 0.1–0.3°K), and contribute an insignificant amount of variance to temperature fluctuations in the tropics. These values correspond to

RMS meridional velocity fluctuations of order 0.3–1.0 m s^{-1} at the equator; values may be much larger at specific times. Planetary MRG modes may contribute substantial variability to the meridional wind field in the tropical upper stratosphere; they in fact dominate the variance in the high-resolution model results reported in Boville and Randel (1991).

Theoretically, there are MRG normal mode oscillations near 29 hours for wave 1 and 39 hours for wave 2 (Hamilton and Garcia 1986), and these are not too far from the frequency bands considered here. The vertical structure of such oscillations should be external, although dissipation may introduce some phase tilt. The vertical wavelengths of order 10–15 km observed here discount significant aliasing from such normal modes.

An interesting feature of these observations is that the periods of the eastward and westward propagating waves are approximately the same (~2.4 days), although the vertical wavelengths differ ($\lambda_z \sim 9$ and 15 km, respectively) following the theoretical dispersion curves. In the model results of Boville and Randel (1991), see Fig. 1, both the periods and wavelengths differ for the eastward and westward wave 1 modes (1.8 and 2.7 days, 17 and 11 km, respectively) again following the dispersion curves. Although the wavelengths and periods are similar for model and observations, the differences in detail suggest that significant differences may exist in the forcing.

The planetary MRG waves observed here contribute less than one-tenth of the zonal accelerations attributable to Kelvin waves observed in the LIMS data. They thus have little significance for the dynamical balances in the tropical middle atmosphere. One possible utility of these observations is in verifying planetary MRG wave spectra in model simulations of the middle atmosphere, and hence validating wave forcing and propagation in such models.

Acknowledgments. The authors thank Rolando Garcia, Eric Fetzer, and Peter Hess for comments and discussions. Reviews by two anonymous referees resulted in significant improvement in presentation of these results. Dan Packman expertly remapped the LIMS data, and Marilena Stone prepared the manuscript. This work has been partially supported under NASA Grant W-16215.

REFERENCES

Andrews, D. G., J. R. Holton and C. B. Leovy, 1987: *Middle Atmosphere Dynamics.* Academic Press, 489 pp.

Boville, B. A., and X. Cheng, 1988: Upper boundary effects in a general circulation model. *J. Atmos. Sci.*, **45,** 2591–2606.

——, and W. J. Randel, 1991: Equatorial waves in a stratospheric GCM: effects of vertical resolution. *J. Atmos. Sci.*, Submitted.

Boyd, J. P., 1978: The effects of latitudinal shear on equatorial waves. Part II: Application to the atmosphere. *J. Atmos. Sci.*, **35,** 2259–2267.

Gille, J. C., and J. M. Russell III, 1984: The Limb Infrared Monitor of the Stratosphere: experiment description, performance, and results. *J. Geophys. Res.*, **89,** 5125–5140.

Hamilton, K., and R. R. Garcia, 1986: Theory and observations of the short-period normal mode oscillations of the atmosphere. *J. Geophys. Res.*, **91,** 11 867–11 875.

——, and J. D. Mahlman, 1988: General circulation model simulation of the semiannual oscillation of the tropical middle atmosphere. *J. Geophys. Res.*, **45,** 3212–3235.

Hayashi, Y., 1982: Space–time spectral analysis and its application to atmospheric waves. *J. Meteorol. Soc. Jpn.*, **60,** 156–171.

Hitchman, M. H., and C. B. Leovy, 1988: Estimation of the Kelvin wave contribution to the semiannual oscillation. *J. Atmos. Sci.*, **45,** 1462–1475.

Holton, J. R., 1975: *The Dynamic Meteorology of the Stratosphere and Mesosphere. Meteor. Monogr.*, No. 37, Amer. Meter. Soc.

——, and R. S. Lindzen, 1972: An updated theory for the quasi-biennial cycle of the tropical stratosphere. *J. Atmos. Sci.*, **29,** 1076–1080.

Rodgers, C. D., 1976: Retrieval of atmospheric temperature and composition from remote measurements of thermal radiation. *Rev. Geophys. Space Phys.*, **14,** 609–624.

Salby, M. L., D. L. Hartmann, P. L. Bailey and J. C. Gille, 1984: Evidence for equatorial Kelvin modes in Nimbus-7 LIMS. *J. Atmos. Sci.*, **41,** 220–235.

Wallace, J. M., 1973: General circulation of the tropical lower stratosphere. *Rev. Geophys. Space Phys.*, **11,** 191–222.

Yanai, M., and T. Maruyama, 1966: Stratospheric wave disturbances propagating over the equatorial Pacific. *J. Meteorol. Soc. Jpn.*, **44,** 291–294.